

Synthesis and structural analysis of the mixed-ligand seven-coordinate complexes $[\text{Ml}_2(\text{CO})_2\{\text{P}(\text{OR})_3\}\{\text{Ph}_2\text{P}(\text{CH}_2)_n\text{PPh}_2\}]$ ($\text{M} = \text{Mo}$, $\text{R} = \text{Me}$, Et , $n = 1$; $\text{R} = \text{Et}$, $i\text{Pr}$, Ph , $n = 2$; $\text{M} = \text{W}$, $\text{R} = \text{Ph}$, $n = 1$; $\text{R} = \text{Me}$, Et , $i\text{Pr}$, $n = 2$). A system where the ligand cone angle and ligand ‘bite’ angle do not affect the coordination geometry

Paul K. Baker ^{a,*}, Michael G.B. Drew ^{b,1}, Archie W. Johans ^b, Ulrike Haas ^a,
Latifah Abdol Latif ^{a,c}, Margaret M. Meehan ^a, Sabrina Zanin ^a

^a Department of Chemistry, University of Wales, Bangor, Gwynedd LL57 2UW, UK

^b Department of Chemistry, University of Reading, Whiteknights, Reading RG6 6AD, UK

^c Centre for Foundation Studies in Science, University of Malaya, 50603 Kuala Lumpur, Malaysia

Received 23 June 1999; received in revised form 15 July 1999

Abstract

Reaction of $[\text{Ml}_2(\text{CO})_3(\text{NCMe})_2]$ with an equimolar amount of $\text{Ph}_2\text{P}(\text{CH}_2)_n\text{PPh}_2$ in CH_2Cl_2 at room temperature gave $[\text{Ml}_2(\text{CO})_3\{\text{Ph}_2\text{P}(\text{CH}_2)_n\text{PPh}_2\}]$, which, followed by an in situ reaction with one equivalent of $\text{P}(\text{OR})_3$, afforded the mixed-ligand seven-coordinate complexes $[\text{Ml}_2(\text{CO})_2\{\text{P}(\text{OR})_3\}\{\text{Ph}_2\text{P}(\text{CH}_2)_n\text{PPh}_2\}]$ ($\text{M} = \text{Mo}$, $\text{R} = \text{Me}$, Et , $n = 1$; $\text{R} = \text{Et}$, $i\text{Pr}$, Ph , $n = 2$; $\text{M} = \text{W}$, $\text{R} = \text{Ph}$, $n = 1$; $\text{R} = \text{Me}$, Et , $i\text{Pr}$, $n = 2$) (1–9) in good yield. All nine complexes have been crystallographically characterised, and they all have surprisingly very similar capped octahedral geometries with a carbonyl group capping an octahedral face containing a carbonyl, the phosphite ligand and one of the phosphorus atoms of the bidentate phosphine ligand. It appears that the different steric effects of the phosphite ligands and angle of bite of the bidentate phosphines do not cause any significant structural differences. © 1999 Elsevier Science S.A. All rights reserved.

Keywords: Seven-coordinate; Molybdenum; Tungsten; Phosphine; Phosphite

1. Introduction

Many seven-coordinate halocarbonyl complexes of the type $[\text{MX}_2(\text{CO})_3\text{L}_2]$ ($\text{M} = \text{Mo}$, W ; $\text{X} = \text{halide}$; $\text{L} = \text{phosphine}$) have been reported [1–16]; however very few complexes of this type or related mixed-ligand complexes containing phosphites have been described. Two examples include $[\text{MoCl}(\text{SnCl}_2^i\text{Bu})(\text{CO})_2\{\text{P}(\text{OMe})_3\}_3]$ [17], and the mixed-ligand complex $[\text{WBr}_2(\text{CO})\{\text{P}(\text{OMe})_3\}_2\{\text{Me}_2\text{AsC}(\text{CF}_3)=\text{C}(\text{CF}_3)\text{AsMe}_2\}]$ [18], which have both been crystallographically characterised.

The structures of seven-coordinate complexes have been shown to be closest to one of the following four geometries: (i) capped octahedral; (ii) capped trigonal prismatic; (iii) pentagonal bipyramidal; or (iv) the so-called 4:3 geometry. Two reviews [19,20] dealing with the structural aspects of seven-coordinate complexes have been published. Hitherto, no detailed structural study of a large series of related seven-coordinate complexes has been made in order to see how steric effects of different ligands affect their structure.

In 1986 [21] we described the synthesis of the highly versatile seven-coordinate complexes $[\text{Ml}_2(\text{CO})_3(\text{NCMe})_2]$ ($\text{M} = \text{Mo}$, W), which have been shown to have a wide range of chemistry [22,23]. In this paper, we describe the synthesis and X-ray crystal structures of

* Corresponding author. Fax: +44-1248-370-528.

¹ Also corresponding author.

Table 1
Physical and analytical data^a for the complexes $[\text{Ml}_2(\text{CO})_2\{\text{P}(\text{OR})_3\}\{\text{Ph}_2\text{P}(\text{CH}_2)_n\text{PPh}_2\}]$ (1–9)

Number	Complex	Colour	Yield (%)	Analysis (%)	
				C	H
1	$[\text{MoI}_2(\text{CO})_2\{\text{P}(\text{OMe})_3\}\{\text{Ph}_2\text{P}(\text{CH}_2)\text{PPh}_2\}]$	Orange	79	39.0 (39.3)	3.5 (3.4)
2	$[\text{MoI}_2(\text{CO})_2\{\text{P}(\text{OEt})_3\}\{\text{Ph}_2\text{P}(\text{CH}_2)\text{PPh}_2\}]$	Orange–brown	65	41.5 (41.5)	3.8 (3.9)
3	$[\text{Wl}_2(\text{CO})_2\{\text{P}(\text{OPh})_3\}\{\text{Ph}_2\text{P}(\text{CH}_2)\text{PPh}_2\}]$	Yellow	60	44.9 (45.5)	3.2 (3.1)
4	$[\text{Wl}_2(\text{CO})_2\{\text{P}(\text{OMe})_3\}\{\text{Ph}_2\text{P}(\text{CH}_2)_2\text{PPh}_2\}]$	Yellow	71	37.1 (36.6)	3.2 (3.3)
5	$[\text{MoI}_2(\text{CO})_2\{\text{P}(\text{OEt})_3\}\{\text{Ph}_2\text{P}(\text{CH}_2)_2\text{PPh}_2\}]$	Yellow–orange	68	41.7 (42.1)	3.8 (4.1)
6	$[\text{Wl}_2(\text{CO})_2\{\text{P}(\text{OEt})_3\}\{\text{Ph}_2\text{P}(\text{CH}_2)_2\text{PPh}_2\}]$	Yellow	65	38.4 (38.6)	3.6 (3.7)
7	$[\text{MoI}_2(\text{CO})_2\{\text{P}(\text{O}^i\text{Pr})_3\}\{\text{Ph}_2\text{P}(\text{CH}_2)_2\text{PPh}_2\}]$	Yellow–orange	82	43.8 (43.8)	4.4 (4.5)
8	$[\text{Wl}_2(\text{CO})_2\{\text{P}(\text{O}^i\text{Pr})_3\}\{\text{Ph}_2\text{P}(\text{CH}_2)_2\text{PPh}_2\}]$	Yellow	51	40.0 (40.4)	4.0 (4.1)
9	$[\text{MoI}_2(\text{CO})_2\{\text{P}(\text{OPh})_3\}\{\text{Ph}_2\text{P}(\text{CH}_2)_2\text{PPh}_2\}]$	Yellow–orange	54	43.9 (43.1)	3.1 (3.5)

^a Calculated values in parentheses.

nine new mixed-ligand mono(phosphite) seven-coordinate complexes $[\text{Ml}_2(\text{CO})_2\{\text{P}(\text{OR})_3\}\{\text{Ph}_2\text{P}(\text{CH}_2)_n\text{PPh}_2\}]$ ($\text{M} = \text{Mo}$, $\text{R} = \text{Me}$, Et , $n = 1$; $\text{R} = \text{Et}$, ^iPr , Ph , $n = 2$; $\text{M} = \text{W}$, $\text{R} = \text{Ph}$, $n = 1$; $\text{R} = \text{Me}$, Et , ^iPr , $n = 2$). The first comparison of a large series of structurally characterised seven-coordinate complexes is also discussed.

2. Results and discussion

2.1. Synthesis and spectroscopic properties of the complexes $[\text{Ml}_2(\text{CO})_2\{\text{P}(\text{OR})_3\}\{\text{Ph}_2\text{P}(\text{CH}_2)_n\text{PPh}_2\}]$

Equimolar quantities of $[\text{Ml}_2(\text{CO})_3(\text{NCMe})_2]$ and $\text{Ph}_2\text{P}(\text{CH}_2)_n\text{PPh}_2$ react in CH_2Cl_2 at room temperature to give the acetonitrile displaced products $[\text{Ml}_2(\text{CO})_3\{\text{Ph}_2\text{P}(\text{CH}_2)_n\text{PPh}_2\}]$, which react in situ with one equivalent of $\text{P}(\text{OR})_3$ to yield the new mixed-ligand seven-coordinate complexes $[\text{Ml}_2(\text{CO})_2\{\text{P}(\text{OR})_3\}\{\text{Ph}_2\text{P}(\text{CH}_2)_n\text{PPh}_2\}]$ ($\text{M} = \text{Mo}$, $\text{R} = \text{Me}$, Et , $n = 1$; $\text{R} = \text{Et}$, ^iPr , Ph , $n = 2$; $\text{M} = \text{W}$, $\text{R} = \text{Ph}$, $n = 1$; $\text{R} = \text{Me}$, Et , ^iPr , $n = 2$) (1–9) via displacement of a carbonyl ligand. Complexes 1–9 have all been characterised by elemental analysis (C, H, N) (Table 1), IR spectroscopy (Table 2), ^1H - and for complexes 4 and 5 ^{31}P -NMR spectroscopy (Tables 3 and 4) and by X-ray crystallography. Complexes 1–9 are all very soluble in polar solvents such as CH_2Cl_2 and CHCl_3 , and reasonably soluble in diethyl ether. The complexes are all air-sensitive in solution, but they can be stored in

the solid state under an inert atmosphere indefinitely. The IR spectra of 1–9 all have two carbonyl bands at ca. 1950 and 1870 cm^{-1} . This indicates that the carbonyl groups are *cis* to each other, which is confirmed by the X-ray crystal structures of 1–9 (see Section 2.2). The ^1H - and selected ^{31}P -NMR spectra also suggest a single isomer in solution. One of the main reasons for carrying out this research was to use the solubilising effect of the phosphite ligands to enable the growth of suitable single crystals of a large series of halocarbonyl complexes, which has proved to be difficult in the past. This was successful, and cooling 4:1 CH_2Cl_2 – Et_2O concentrated solutions of 1–9 to -20°C gave suitable single crystals for X-ray crystallography of all nine complexes.

Table 2
Infrared spectral data^a for the complexes $[\text{Ml}_2(\text{CO})_2\{\text{P}(\text{OR})_3\}\{\text{Ph}_2\text{P}(\text{CH}_2)_n\text{PPh}_2\}]$ (1–9)

Complex	$\nu(\text{C}=\text{O})$ ^a (cm^{-1})
1	1955(s); 1881(s)
2	1951(s); 1879(s)
3	1953(s); 1877(s)
4	1937(s); 1859(s)
5	1950(s); 1874(s)
6	1940(s); 1860(s)
7	1948(s); 1874(s)
8	1937(s); 1860(s)
9	1958(s); 1867(s)

^a Run as thin CHCl_3 films between NaCl plates: s, strong.

Table 3
 $^1\text{H-NMR}$ data (δ)^a for the complexes
 $[\text{Ml}_2(\text{CO})_2\{\text{P}(\text{OR})_3\}\{\text{Ph}_2\text{P}(\text{CH}_2)_n\text{PPh}_2\}]$ (1–9)

Complex	$^1\text{H-NMR}$ data: δ (ppm) J (Hz)
1	7.8–7.2 (m, 20H, Ph-H), 5.3 (t, 2H, $J_{\text{P-H}} = 8.5$ Hz, PCH_2P), 3.8 {d, 9H, $J_{\text{P-H}} = 11.8$ Hz, $\text{P}(\text{OCH}_3)_3$ }
2	7.8–7.2 (m, 20H, Ph-H), 5.35 (t, 2H, $J_{\text{P-H}} = 8.0$ Hz, PCH_2P), 4.2 [m, 6H, $\text{P}(\text{OCH}_2\text{CH}_3)_3$], 1.3 [t, 9H, $J_{\text{H-H}} = 7.7$ Hz, $\text{P}(\text{OCH}_2\text{CH}_3)_3$]
3	8.0–7.2 (m, 35H, Ph-H), 5.7 (t, 2H, $J_{\text{P-H}} = 22.4$ Hz, PCH_2P)
4	8.0–7.3 (m, 20H, Ph-H), 3.65 {d, 9H, $J_{\text{P-H}} = 8.5$ Hz, $\text{P}(\text{OCH}_3)_3$ }, 2.2 (m, 4H, $\text{PCH}_2\text{CH}_2\text{P}$)
5	8.0–7.2 (m, 20H, Ph-H), 4.1 [m, 6H, $\text{P}(\text{OCH}_2\text{CH}_3)_3$], 3.35, 2.25 (br, 4H, $\text{PCH}_2\text{CH}_2\text{P}$), 1.2 [t, 9H, $J_{\text{H-H}} = 7.7$ Hz, $\text{P}(\text{OCH}_2\text{CH}_3)_3$]
6	8.0–7.4 (m, 20H, Ph-H), 4.2 [m, 6H, $\text{P}(\text{OCH}_2\text{CH}_3)_3$], 2.9 (br, 4H, $J_{\text{P-H}} = 7.7$ Hz, $\text{PCH}_2\text{CH}_2\text{P}$), 1.4 [t, 9H, $J_{\text{H-H}} = 7.3$ Hz, $\text{P}(\text{OCH}_2\text{CH}_3)_3$]
7	8.0–7.2 (m, 20H, Ph-H), 4.9 [brm, 3H, $\text{P}\{\text{OCH}(\text{CH}_3)_2\}_3$], 2.3 (brm, 4H, $\text{PCH}_2\text{CH}_2\text{P}$), 1.3 [m, 18H, $\text{P}\{\text{OCH}(\text{CH}_3)_2\}_3$]
8	8.0–7.3 (m, 20H, Ph-H), 4.75 [brm, 3H, $\text{P}\{\text{OCH}(\text{CH}_3)_2\}_3$], 2.5 (brm, 4H, $\text{PCH}_2\text{CH}_2\text{P}$), 1.25 [m, 18H, $\text{P}\{\text{OCH}(\text{CH}_3)_2\}_3$]
9	8.1–7.0 (m, 35H, Ph-H), 2.8 (br, 4H, $\text{PCH}_2\text{CH}_2\text{P}$)

^a Samples run in CDCl_3 , with SiMe_4 as external standard at 25°C: d, doublet; t, triplet; m, multiplet; br, broad.

Table 4
 $^{31}\text{P}\{-^1\text{H}\}$ -NMR data^a for selected complexes
 $[\text{Ml}_2(\text{CO})_2\{\text{P}(\text{OR})_3\}\{\text{Ph}_2\text{P}(\text{CH}_2)_n\text{PPh}_2\}]$ (4) and (5)

Complex	$^{31}\text{P}\{-^1\text{H}\}$ data: δ (ppm)
4	100.8 {dd, 1P, $^2J_{\text{P-P}} = 17.5$ Hz <i>cis</i> , $J_{\text{P-P}} = 224$ Hz <i>trans</i> , $\text{P}(\text{OCH}_3)_3$ }, 43.9 (t, 1P, $J_{\text{P-P}} = 20.1$ Hz <i>cis</i> , $J_{\text{W-P}} = 196.7$ Hz, $\text{PCH}_2\text{CH}_2\text{P}$), 3.4 {dd, 1P, $^2J_{\text{P-P}} = 17.5$ Hz, <i>cis</i> , $^1J_{\text{P-P}} = 224$ Hz, <i>trans</i> , $J_{\text{W-P}} = 304$ Hz, $\text{PCH}_2\text{CH}_2\text{P}$ }
5	125.2 {dd, br <i>cis</i> , 1P, $J_{\text{P-P}} = 236.7$ Hz <i>trans</i> , $\text{P}(\text{OEt})_3$ }, 66.8 {t, 1P, $J_{\text{P-P}} = 30.1$ Hz, <i>cis</i> , $\text{PCH}_2\text{CH}_2\text{P}$ }, 22.9 {dd, 1P, $^2J_{\text{P-P}} = 30.1$ Hz <i>cis</i> , $^1J_{\text{P-P}} = 230.1$ Hz, <i>trans</i> - $\text{PCH}_2\text{CH}_2\text{P}$ }

^a Spectra recorded in CDCl_3 (+25°C) and referenced to 85% H_3PO_4 : br, broad; dd, doublet of doublets; t, triplet.

2.2. Crystal structures of $[\text{Ml}_2(\text{CO})_2\{\text{P}(\text{OR})_3\}\{\text{Ph}_2\text{P}(\text{CH}_2)_n\text{PPh}_2\}]$ (1–9) and a discussion of how *R* and *n* affect the structures of these complexes

The nine structures are shown in Figs. 1–9, respectively, together with the common numbering scheme. Similar projections have been chosen so that the remarkable similarity of the structures is readily apparent. The metal atoms are seven-coordinate, being bonded to two carbonyl groups, two iodine atoms, a phosphite ligand and a bidentate phosphine ligand, either dppm or dppe. The environment of the metal

atom in all nine complexes can best be considered to be a capped octahedron with C(100) in the capping position, C(200), the phosphite P(7) and one phosphorus P(6) of the bidentate ligand in the capped face and the remaining phosphorus of the bidentate ligand and the two iodine atoms in the uncapped face.

The bond lengths for the comparable bonds in all nine compounds are very similar. There is very little difference in size between molybdenum and tungsten and variations are within standard deviations. For example, there are five structures containing Mo and four containing W and average Mo–I and W–I distances are 2.995 and 2.989 Å, respectively.

In all structures the bond length from the metal to the phosphorus atom in the uncapped face (this is called P(3) for the dppe ligand and P(4) for the dppm ligand) is longer by ca. 0.1 Å than that to the atom P(6) in the capped face. This could be due to crowding in the uncapped face, or perhaps the *trans* effect of the phosphite ligand. It is noticeable that the M–P(3) distance (dppe ligand) is significantly longer (six examples, mean 2.647 Å) than the M–P(4) distance (dppm ligand) (three examples, mean 2.599 Å). There is a similar, but barely significant differential between the M–P(7) distances (2.495 Å in dppm, 2.505 Å in dppe).

When the angles are considered, the major difference is between the dppm bite (average 65.7°) and the dppe bite (average 75.2°). Four different $\text{P}(\text{OR})_3$ phosphite ligands are used in the formation of these complexes with R = Me, Et, ⁱPr and Ph. It has been suggested that the different substituents may affect the electronic and steric effects of the ligands. The steric effects have been quantified by the cone angle [24]. However, there is no variation between the bond lengths of either the M–P(7) bond, or the mutually *trans* bond that can be correlated with any difference in R. Cone angles for R = Me, Et, ⁱPr and Ph have been calculated to be 107, 109, 128 and 130° [24].

We have investigated possible changes in dimensions that could be correlated with the change in R and the proposed cone angle. One likely dimension was thought to be the I–M–P(7)–O(*n*) torsion angles (*n* = 7, 8, 9) and these are shown in Table 7, but these just showed the remarkable similarity in the structures. Torsion angles remained within 40° of each other. It is noticeable that the bulkiest substituent R = ⁱPr has the most staggered torsion angle, but in general the angles cannot be correlated with the size of R.

We next looked at the angles subtended at the metal by the phosphite ligand. Clearly, if the cone angle has any serious effect on geometry, then this is particularly likely to occur for the *cis* angles C(100)–M–P(7), I(2)–M–P(7) and I(3)–M–P(7). However, no such effect is apparent and the overall impression from this set of structures is that there is no significant effect of change in R on the geometry of the complexes.

These cone-angle calculations [24] may be less significant in the case of the phosphite ligand than in the case of some other ligands for which cone-angle differences have been found to be significant, because it is always possible for the alkyl groups in the phosphite ligands to

rotate to reduce steric effects. Another factor is that the P–O–C angles can vary significantly. However, again there is no correlation; average angles being (1) Me 129; (2) Et 122; (3) Ph 130; (4) Et 120, 124; (5) ⁱPr 132; (6) Me 139; (7) ⁱPr 131; (8) Et 125; and (9) Ph 129°.

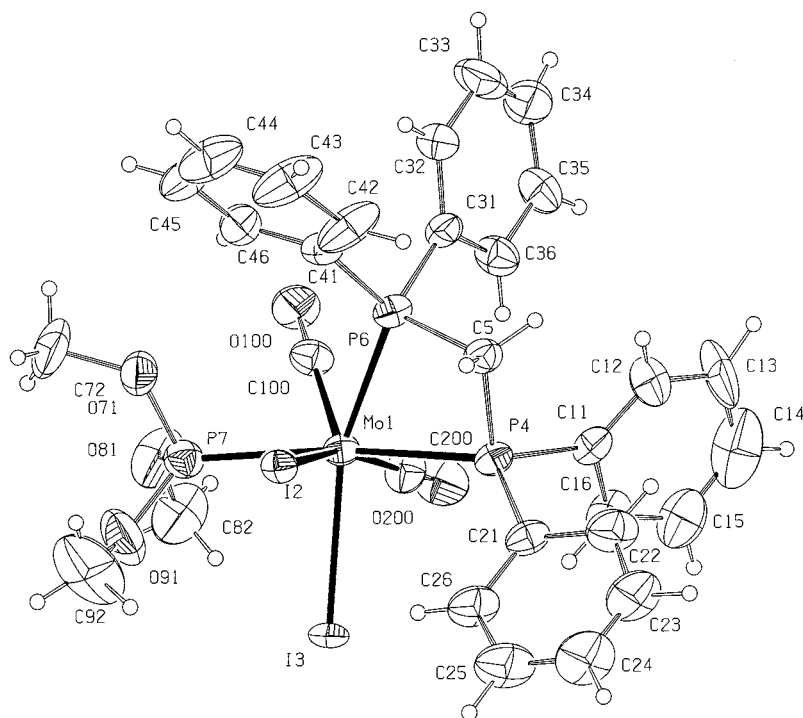


Fig. 1. The structure of **1** with the atomic numbering scheme. Ellipsoids shown at 30% occupancy.

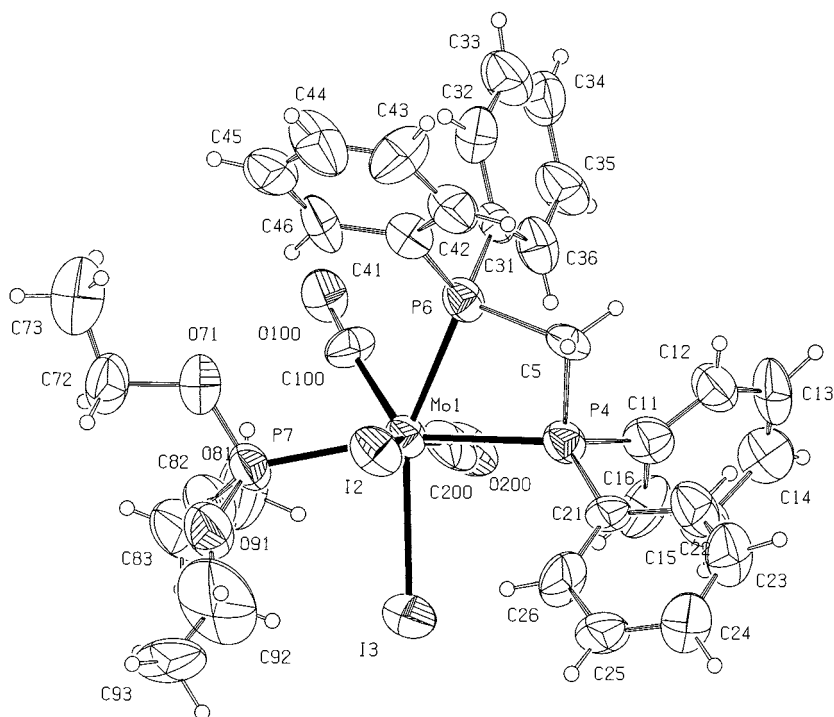


Fig. 2. The structure of **2** with the atomic numbering scheme. Ellipsoids shown at 30% occupancy.

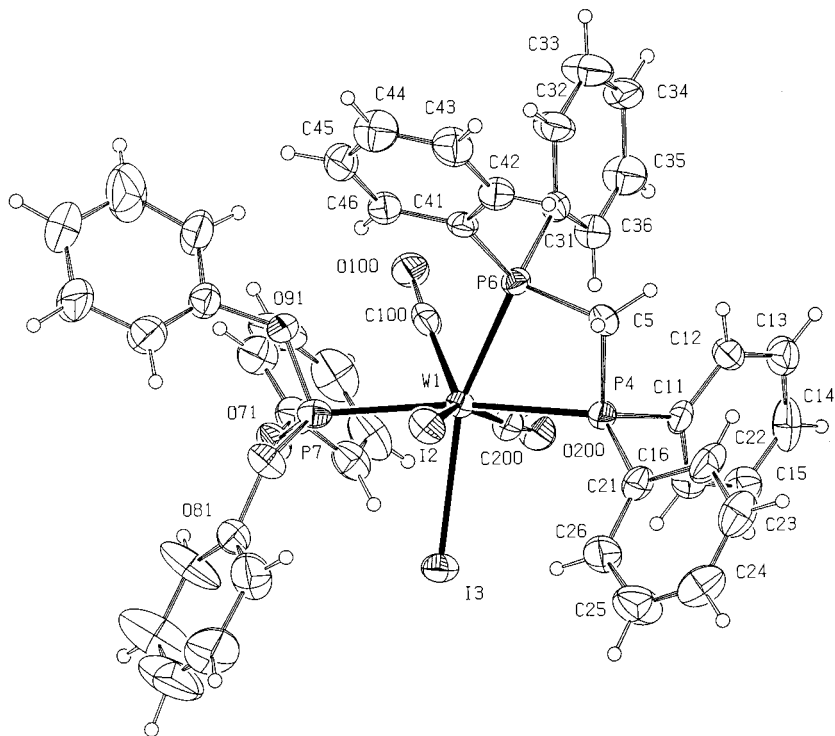


Fig. 3. The structure of **3** with the atomic numbering scheme. Ellipsoids shown at 30% occupancy.

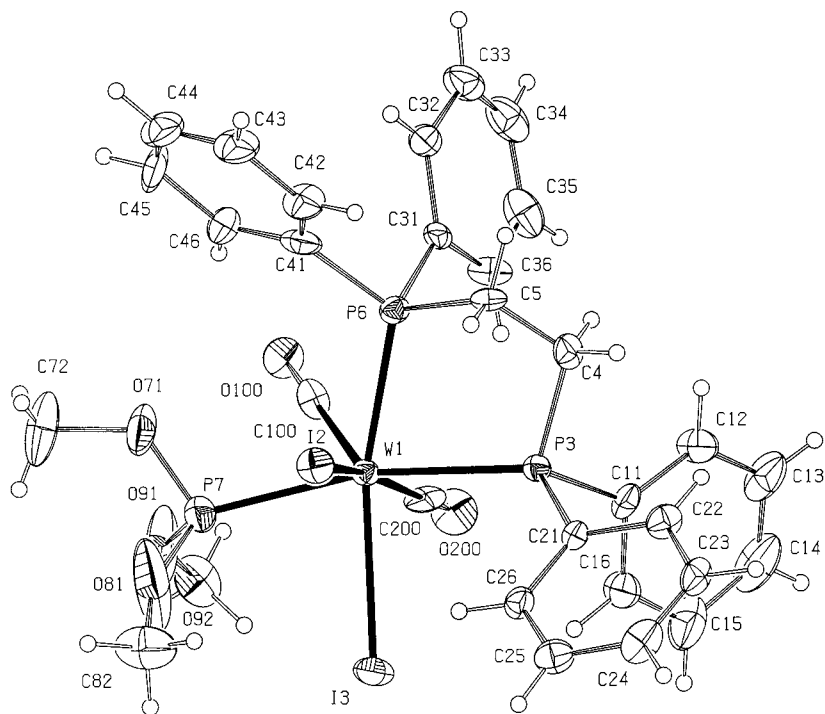


Fig. 4. The structure of **4** with the atomic numbering scheme. Ellipsoids shown at 30% occupancy.

The size of the R groups has in fact made little difference to the shape of the coordination sphere although, as is apparent from the Figures, the phosphite groups are on the opposite side of the coordination

sphere to the bidentate phosphorus ligands and the small carbonyl groups are their nearest neighbours. With alkyl groups such as R = Me, Et, ⁱPr the contacts with the rest of the coordination sphere are well above

the sum of van der Waals radii. However, with $R = \text{Ph}$, some close contacts are apparent. In structures **3** and **9**, it is found that the plane of one phenyl ring is approximately parallel to the plane of the $\text{M}(\text{CO})_2$ moiety,

thus avoiding closer contacts. Even so, closest distances with carbonyl oxygen atoms and ring carbons are 3.29 (in **3**) and 3.07 (in **9**). By contrast, the closest similar contact in **8** (with $R = ^i\text{Pr}$) is 3.55 Å.

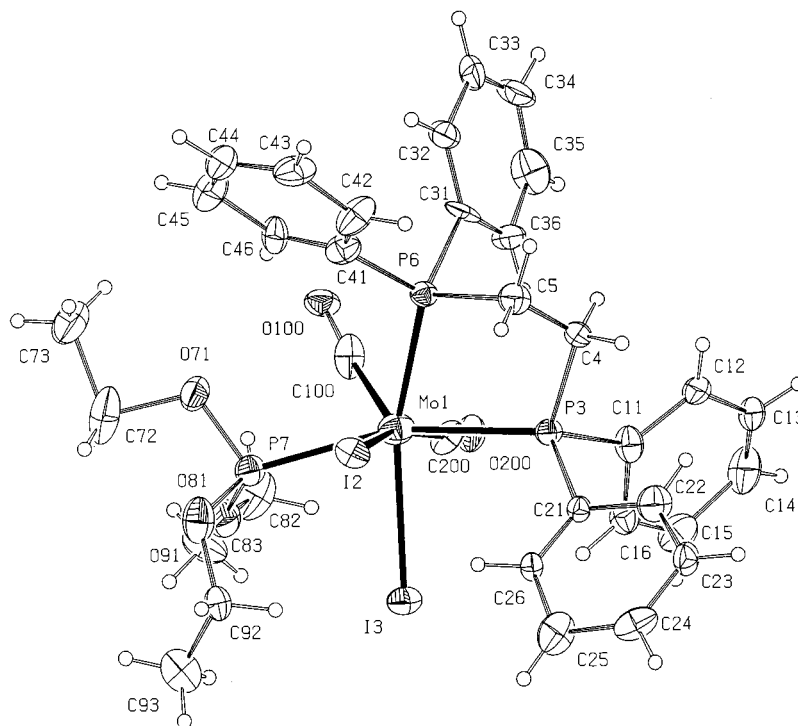


Fig. 5. The structure of **5** with the atomic numbering scheme. Ellipsoids shown at 30% occupancy.

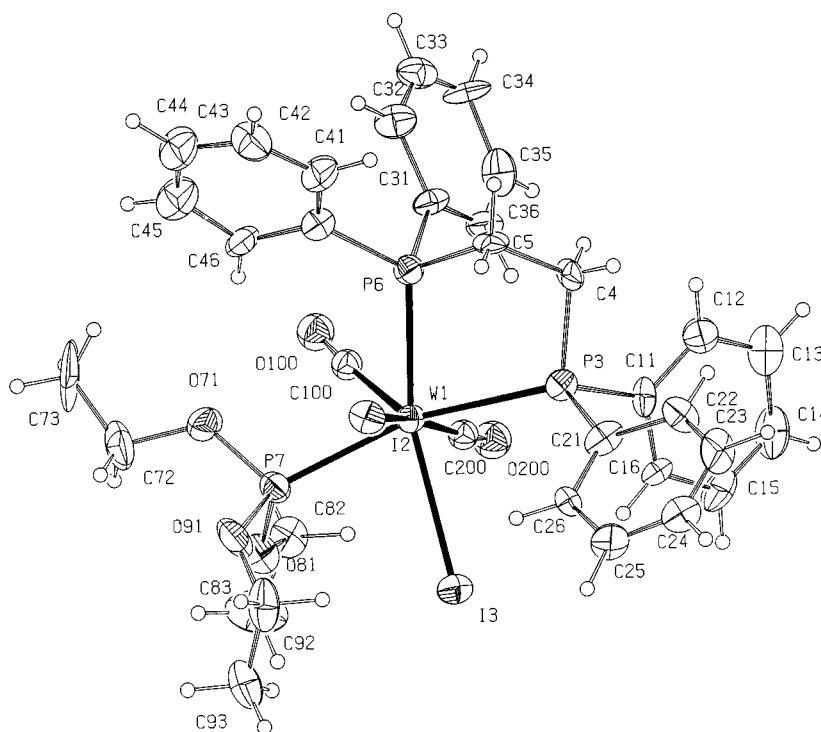


Fig. 6. The structure of **6** with the atomic numbering scheme. Ellipsoids shown at 30% occupancy.

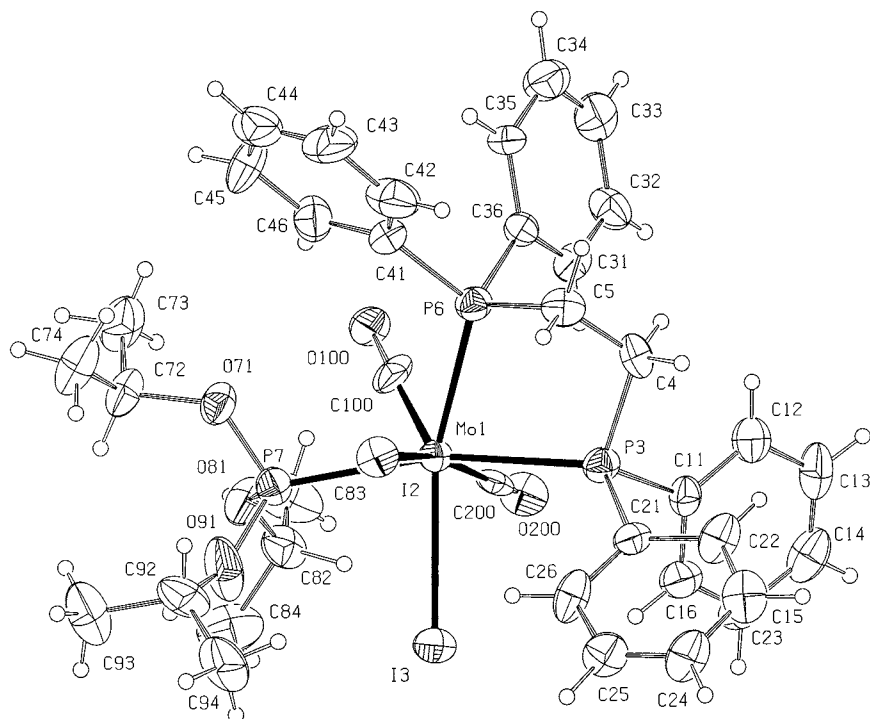


Fig. 7. The structure of **7** with the atomic numbering scheme. Ellipsoids shown at 30% occupancy.

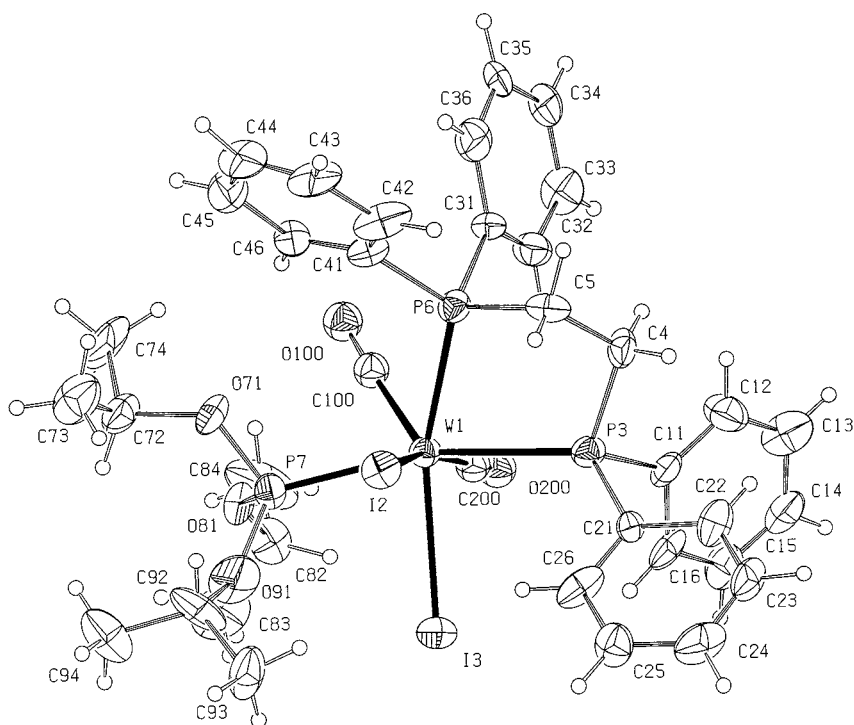


Fig. 8. The structure of **8** with the atomic numbering scheme. Ellipsoids shown at 30% occupancy.

2.3. Conclusions

We can only conclude that for the structures reported here the cone angle has no effect on the structures and that the slight variations observed are much more likely

to be due to packing effects. The range of cone angles [24] considered in this study with phosphite ligands from 107 to 130° is small compared with the wide range angles for monodentate phosphine ligands available, and will be the subject of another study. The choice of

highly solubilising phosphite ligands in this study has enabled growth of nine suitable single crystals for X-ray analysis, which may be more difficult with monodentate phosphine ligands.

3. Experimental

All reactions described in this paper were carried out under an atmosphere of dry dinitrogen using standard vacuum/Schlenk-line techniques. The starting materials, $[\text{MI}_2(\text{CO})_3(\text{NCMe})_2]$ ($\text{M} = \text{Mo}, \text{W}$), were prepared according to the literature method [21]. The solvents used in this research, CH_2Cl_2 and diethyl ether, were dried and distilled before use. All chemicals used were purchased from commercial sources.

Elemental analyses (C, H and N) were determined by Glyn Connolly (Department of Chemistry, University of Wales, Bangor, Gwynedd, LL57 2UW) using a Carlo Erba Elemental Analyser MOD1108 (using helium as a carrier gas). Infrared spectra were recorded as thin CHCl_3 films between NaCl plates on a Perkin–Elmer 1600 series FTIR spectrophotometer. ^1H - (referenced to SiMe_4) and ^{31}P - (referenced to 85% H_3PO_4) NMR spectra were recorded on a Bruker AC250 MHz NMR spectrometer.

3.1. Syntheses

3.1.1. $[\text{MoI}_2(\text{CO})_2\{\text{P}(\text{OEt})_3\}\{\text{Ph}_2\text{P}(\text{CH}_2)\text{PPh}_2\}]$ (**2**)

In a typical reaction, to a stirred solution of $[\text{MoI}_2(\text{CO})_3(\text{NCMe})_2]$ (0.5 g, 0.969 mmol) in CH_2Cl_2 (30 cm^3) under a stream of dry N_2 was added $\text{Ph}_2\text{P}(\text{CH}_2)\text{PPh}_2$ (0.372 g, 0.969 mmol). After 10 min of stirring, $\text{P}(\text{OEt})_3$ (0.161 g, 0.969 mmol) was added. Filtration through Celite, followed by removal of the solvent after 20 min, yielded a yellowish–orange product. Recrystallisation from 4:1 CH_2Cl_2 – Et_2O at -20°C afforded analytically pure orange–brown crystals of $[\text{MoI}_2(\text{CO})_2\{\text{P}(\text{OEt})_3\}\{\text{Ph}_2\text{P}(\text{CH}_2)\text{PPh}_2\}]$ (**2**) (0.603 g, 65%) which were suitable for X-ray crystallography. Compounds **1**, **5**, **7** and **9** were prepared in an analogous manner. For the tungsten complexes, **3**, **4**, **6** and **8**, an analogous procedure was followed, but the mixture was stirred for 1 h instead of 20 min as for the molybdenum complexes.

3.1.2. Crystallography — crystal structure determination

Suitable single crystals for X-ray crystallography for the complexes $[\text{MI}_2(\text{CO})_2\{\text{P}(\text{OR})_3\}\{\text{Ph}_2\text{P}(\text{CH}_2)_n\text{PPh}_2\}]$ (**1–9**) were all grown by cooling concentrated 4:1 CH_2Cl_2 – Et_2O solutions of **1–9** to -20°C for 24 h.

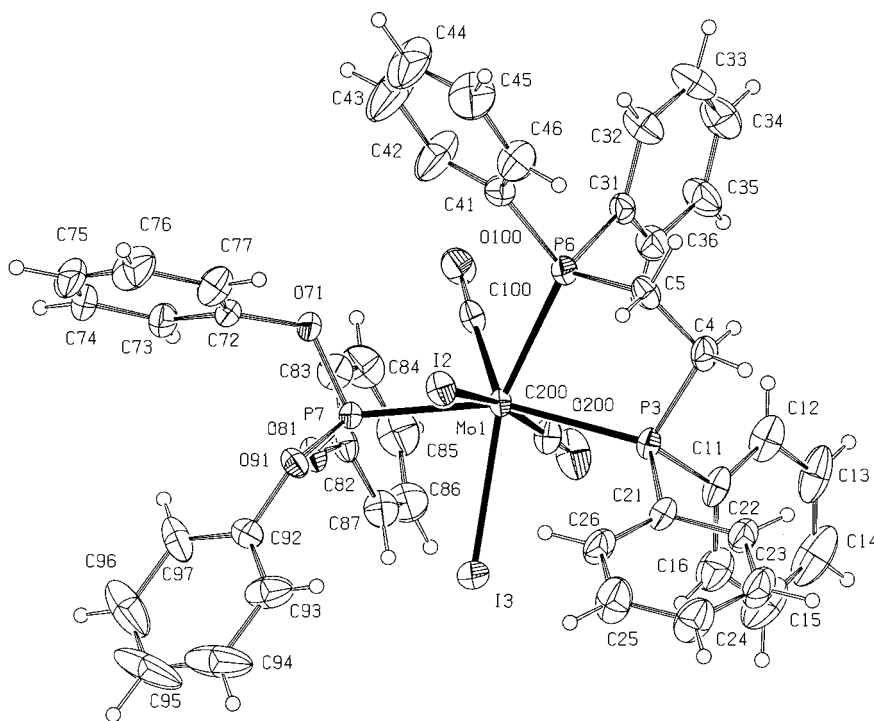


Fig. 9. The structure of **9** with the atomic numbering scheme. Ellipsoids shown at 30% occupancy.

Table 5
Crystal data and structure refinement details for the structures

	1	2	3	4	5	6	7	8	9
Formula	MoI ₂ (CO) ₂ (P(OMe) ₃) (dppm)	MoI ₂ (CO) ₂ (P(OEt) ₃)(dppm)	WI ₂ (CO) ₂ (P(OPh) ₃)(dppm), 2H ₂ O	WI ₂ (CO) ₂ (P(OMe) ₃)(dppe)	MoI ₂ (CO) ₂ (P(OEt) ₃)(dppe)	WI ₂ (CO) ₂ (P(OEt) ₃)(dppe)	MoI ₂ (CO) ₂ (P(OPr) ₃)(dppe)	WI ₂ (CO) ₂ (P(OPr) ₃)(dppe)	MoI ₂ (CO) ₂ (P(OPh) ₃)(dppe)
Empirical formula	C ₃₀ H ₃₁ I ₂ MoO ₅ P ₃	C ₃₃ H ₃₇ I ₂ MoO ₅ P ₃	C ₄₅ H ₃₇ I ₂ O ₇ P ₃ W	C ₃₄ H ₃₉ I ₂ MoO ₅ P ₃	C ₃₁ H ₃₃ I ₂ O ₅ P ₃ W	C ₃₄ H ₃₉ I ₂ O ₅ P ₃ W	C ₃₇ H ₄₅ I ₂ MoO ₅ P ₃	C ₃₇ H ₄₅ I ₂ O ₅ P ₃ W	C ₄₆ H ₃₉ I ₂ MoO ₅ P ₃
Formula weight	914.20	956.27	1220.31	1016.13	970.30	1008.21	1012.38	1100.29	1114.42
Crystal system	Monoclinic	Monoclinic	Monoclinic	Monoclinic	Triclinic	Monoclinic	Monoclinic	Monoclinic	Monoclinic
Space group	<i>P</i> 2 ₁ / <i>n</i>	<i>C</i> 2/ <i>c</i>	<i>P</i> 2 ₁ / <i>c</i>	<i>P</i> 2 ₁ / <i>c</i>	<i>P</i> $\bar{1}$	<i>C</i> 2/ <i>c</i>	<i>P</i> 2 ₁ / <i>c</i>	<i>P</i> 2 ₁ / <i>c</i>	<i>P</i> 2 ₁ / <i>n</i>
Unit cell dimensions									
<i>a</i> (Å)	11.361(9)	35.10(4)	13.313(14)	16.59(2)	10.207(11)	36.55(4)	18.351(17)	18.346(19)	11.723(14)
<i>b</i> (Å)	11.484(12)	10.485(13)	17.45(2)	10.081(14)	18.924(22)	10.131(12)	10.457(12)	10.440(12)	23.86(3)
<i>c</i> (Å)	26.36(3)	21.82(2)	20.65(2)	20.52(2)	21.556(25)	21.53(2)	21.14(2)	21.13(2)	17.26(2)
α (°)	(90)	(90)	(90)	(90)	70.5(1)	(90)	(90)	(90)	(90)
β (°)	95.25(1)	107.35(1)	98.16(1)	91.23(1)	89.1(1)	110.38(1)	91.02(1)	91.15(1)	95.71(1)
γ (°)	(90)	(90)	(90)	(90)	74.2(1)	(90)	(90)	(90)	(90)
<i>V</i> (Å ³)	3425(6)	7665(15)	4748(9)	3432(7)	3764(8)	7474(15)	4055(7)	4045(8)	4802(10)
<i>Z</i>	4	8	4	4	2	8	4	4	4
<i>D</i> _{calc.} (g cm ⁻³)	1.773	1.657	1.707	1.967	1.712	1.881	1.658	1.807	1.541
Absorption coefficient (mm ⁻¹)	2.361	2.111	3.880	5.342	2.154	4.909	2.003	4.539	1.700
<i>F</i> (000)	1776	3744	2352	1936	1904	4064	2000	2128	2192
Crystal size (mm)	0.30 × 0.25 × 0.20	0.25 × 0.20 × 0.20	0.25 × 0.20 × 0.25	0.25 × 0.20 × 0.10	0.32 × 0.25 × 0.12	0.35 × 0.22 × 0.21	0.30 × 0.25 × 0.20	0.25 × 0.25 × 0.20	0.25 × 0.25 × 0.20
θ range for data collection (°)	2.36–25.95	3.02–26.34	2.31–25.97	2.25–25.90	2.17–25.93	3.43–25.32	2.27–25.93	2.21–26.06	2.79–26.10
Index ranges	0 ≤ <i>h</i> ≤ 12, –12 ≤ <i>k</i> ≤ 12, –32 ≤ <i>l</i> ≤ 32	0 ≤ <i>h</i> ≤ 43, –11 ≤ <i>k</i> ≤ 10, –26 ≤ <i>l</i> ≤ 21	0 ≤ <i>h</i> ≤ 16, –21 ≤ <i>k</i> ≤ 21, –23 ≤ <i>l</i> ≤ 23	–0 ≤ <i>h</i> ≤ 20, –10 ≤ <i>k</i> ≤ 10, –15 ≤ <i>l</i> ≤ 25	–12 ≤ <i>h</i> ≤ 12, –21 ≤ <i>k</i> ≤ 23, 0 ≤ <i>l</i> ≤ 26	0 ≤ <i>h</i> ≤ 44, –11 ≤ <i>k</i> ≤ 11, –26 ≤ <i>l</i> ≤ 17	–22 ≤ <i>h</i> ≤ 22, 0 ≤ <i>k</i> ≤ 8, –23 ≤ <i>l</i> ≤ 23	–22 ≤ <i>h</i> ≤ 22, 0 ≤ <i>k</i> ≤ 8, –23 ≤ <i>l</i> ≤ 23	0 ≤ <i>h</i> ≤ 14, –28 ≤ <i>k</i> ≤ 20, –21 ≤ <i>l</i> ≤ 19
Reflections collected	7804	8338	14 031	9961	8737	7145	8249	10 266	16 703
Unique reflections	4762	5481	7937	5676		4669	4730	5654	8760
	[<i>R</i> _{int} = 0.0322]	[<i>R</i> _{int} = 0.0838]	[<i>R</i> _{int} = 0.0458]	[<i>R</i> _{int} = 0.0535]		[<i>R</i> _{int} = 0.0520]	[<i>R</i> _{int} = 0.0604]	[<i>R</i> _{int} = 0.1033]	[<i>R</i> _{int} = 0.0314]
Data/restraints/parameters	4762/0/374	5431/0/400	7937/0/514	5676/0/383	8737/96/817	4669/36/390	4730/0/440	5654/36/420	8760/0/515
Final <i>R</i> indices [<i>I</i> > 2σ(<i>I</i>)]									
<i>R</i> ₁	0.0494	0.1239	0.0593	0.0662	0.0673	0.1042	0.0843	0.0854	0.0512
<i>wR</i> ₂	0.1509	0.3261	0.1730	0.1502	0.1835	0.2736	0.2207	0.2134	0.1071
<i>R</i> indices (all data)									
<i>R</i> ₁	0.0688	0.1970	0.0899	0.0998	0.1138	0.1305	0.1205	0.1556	0.0756
<i>wR</i> ₂	0.1800	0.3847	0.1992	0.1654	0.2033	0.2988	0.2367	0.2592	0.1179
Largest difference peak and hole (e Å ⁻³)	1.568 and –1.030	1.128 and –0.981	2.033 and –2.057	1.539 and –1.363	1.046 and –0.884	2.578 and –2.313	1.112 and –0.804	3.392 and –1.904	1.142 and 0.743

Table 6
Molecular dimensions

	1	2	3	4	5a	5b	6	7	8	9
<i>Bond lengths</i>										
M(1)–C(100)	1.945(8)	1.953(19)	1.969(14)	1.952(17)	1.898(16)	1.892(15)	2.00(2)	1.94(2)	2.00(2)	1.945(7)
M(1)–C(200)	1.978(9)	1.97(3)	1.970(13)	1.966(16)	1.983(13)	1.929(17)	1.94(2)	1.98(2)	1.93(2)	1.962(7)
M(1)–P(7)	2.484(3)	2.506(6)	2.495(4)	2.490(5)	2.537(5)	2.513(4)	2.501(7)	2.528(5)	2.517(6)	2.453(2)
M(1)–P(6)	2.498(3)	2.497(6)	2.501(3)	2.497(4)	2.520(5)	2.503(5)	2.509(7)	2.510(6)	2.514(6)	2.525(3)
M(1)–P(<i>n</i>) ^a	2.605(3)	2.604(6)	2.587(3)	2.628(5)	2.655(4)	2.665(4)	2.649(7)	2.651(5)	2.643(6)	2.633(3)
M(1)–I(2)	2.872(3)	2.876(3)	2.856(3)	2.874(3)	2.896(3)	2.916(3)	2.887(3)	2.904(3)	2.891(3)	2.872(2)
M(1)–I(3)	2.886(2)	2.890(3)	2.882(2)	2.898(3)	2.936(3)	2.932(3)	2.918(3)	2.908(3)	2.900(3)	2.916(3)
<i>Bond angles</i>										
C(100)–M(1)–C(200)	72.8(4)	75.2(11)	73.8(5)	69.9(6)	69.8(6)	73.6(6)	69.9(9)	72.7(7)	70.0(9)	74.3(3)
C(100)–M(1)–P(7)	71.0(3)	71.5(7)	73.2(3)	73.0(5)	72.9(5)	71.8(4)	72.4(7)	71.4(7)	71.9(7)	75.2(2)
C(200)–M(1)–P(7)	108.7(3)	107.8(7)	109.7(3)	108.8(5)	106.9(4)	107.1(4)	106.9(7)	105.5(5)	104.8(6)	105.0(2)
C(100)–M(1)–P(6)	74.0(3)	71.7(5)	73.2(3)	72.9(6)	72.9(6)	71.8(4)	73.8(8)	71.9(6)	72.8(6)	71.5(2)
C(200)–M(1)–P(6)	109.8(3)	104.4(7)	109.6(3)	109.6(4)	110.2(5)	110.9(4)	109.8(7)	111.0(5)	110.0(6)	111.1(2)
P(7)–M(1)–P(6)	115.8(1)	121.8(2)	117.1(1)	114.1(1)	117.1(1)	115.9(1)	116.1(2)	116.0(2)	115.7(2)	120.7(1)
C(100)–M(1)–P(<i>n</i>) ^a	122.8(3)	126.6(7)	122.7(3)	125.7(5)	124.7(5)	127.0(4)	127.0(7)	124.5(7)	124.0(7)	127.1(2)
C(200)–M(1)–P(<i>n</i>) ^a	84.6(3)	84.9(7)	84.4(3)	81.0(5)	81.2(4)	80.7(4)	81.7(7)	79.4(5)	81.0(6)	80.5(2)
P(7)–M(1)–P(<i>n</i>) ^a	164.0(1)	161.0(2)	162.1(1)	161.3(1)	160.5(1)	161.1(1)	160.5(2)	163.8(2)	163.9(2)	157.3(1)
P(6)–M(1)–P(<i>n</i>) ^a	65.5(1)	66.1(2)	65.6(1)	75.4(1)	74.7(1)	75.4(1)	75.5(2)	75.0(2)	74.9(2)	75.7(1)
C(100)–M(1)–I(2)	125.9(3)	118.6(7)	128.8(3)	125.5(5)	125.4(4)	121.0(5)	124.7(7)	123.1(6)	125.0(6)	118.2(2)
C(200)–M(1)–I(2)	161.3(3)	165.9(8)	157.4(3)	164.6(4)	164.8(5)	165.4(4)	165.5(6)	164.1(5)	165.0(6)	167.4(2)
P(7)–M(1)–I(2)	81.4(1)	81.0(2)	82.2(1)	79.9(1)	80.0(1)	80.3(1)	80.4(2)	81.5(1)	81.3(1)	78.1(1)
P(6)–M(1)–I(2)	78.0(1)	79.0(2)	79.7(1)	76.7(1)	77.2(1)	75.6(1)	76.7(2)	77.2(1)	77.4(1)	76.4(1)
P(<i>n</i>) ^a –M(1)–I(2)	83.4(1)	84.0(2)	81.0(1)	87.3(1)	88.3(1)	88.6(1)	87.7(2)	90.1(1)	89.7(1)	92.2(1)
C(100)–M(1)–I(3)	129.1(3)	132.6(5)	128.8(3)	125.9(4)	124.5(5)	126.5(4)	124.8(8)	127.8(6)	127.3(6)	132.3(2)
C(200)–M(1)–I(3)	76.4(3)	78.2(8)	76.4(3)	77.5(4)	75.1(5)	74.8(4)	76.3(7)	75.4(5)	76.5(3)	76.9(2)
P(7)–M(1)–I(3)	82.0(1)	80.5(2)	79.1(1)	78.5(1)	76.1(1)	77.7(1)	77.5(2)	78.9(1)	79.0(1)	76.5(1)
P(6)–M(1)–I(3)	156.0(1)	153.9(1)	157.4(1)	160.8(1)	161.8(1)	161.1(1)	160.9(1)	159.7(1)	159.4(1)	155.7(1)
P(<i>n</i>) ^a –M(1)–I(3)	92.9(1)	88.6(2)	94.2(1)	88.5(1)	89.3(1)	88.2(1)	87.9(2)	87.8(1)	87.9(1)	83.5(1)
I(2)–M(1)–I(3)	89.9(1)	92.7(1)	87.5(1)	92.2(1)	93.9(1)	95.0(1)	93.5(1)	92.5(1)	91.5(7)	92.2(1)

^a Called P(4) in dpmp, P(3) in dppe.

Crystal data for the nine structures are given in Table 5, together with refinement details. Bond lengths and angles for the metal coordination spheres of **1**–**9** are given in Table 6. For all compounds, data were collected with Mo–K α radiation using the MarResearch Image Plate System. The crystals were positioned at 70 mm from the Image Plate. Ninety-five frames were positioned at

Table 7
Torsion angles I(2)–M–P(7)–O(*n*1), for *n* = 7, 8 and 9

Structure	Angles (°)			R in phosphite
	<i>n</i> = 7	<i>n</i> = 8	<i>n</i> = 9	
1	70.3	–178.6	–60.0	Me
2	81.2	–158.7	–36.6	Et
3	86.4	–154.3	–28.6	Ph
4	73.2	–171.8	–46.7	Me
5a	88.4	–150.0	–21.4	Et
5b	87.5	–151.3	–24.6	Et
6	88.3	–148.5	–26.7	Et
7	70.0	–177.1	–61.0	^t Pr
8	70.8	–174.9	–62.5	^t Pr
9	77.9	–161.5	–38.0	Ph

2° intervals with a counting time of 2 min. Compounds **2** and **6** were isomorphous, as were **7** and **8**. Data analyses were carried out with the XDS program. [25] The structures were solved using direct methods with the SHELXL 86 program [26]. In **5** there were two molecules in the asymmetric unit. There were no solvent molecules in any of the structures apart from **3**, where two water molecules were located. In **2**, one of the phosphite ethyl groups was disordered and two positions were refined with 50% occupancy. In all structures, the non-hydrogen atoms were refined with anisotropic thermal parameters apart from the water molecules in **3** and the carbonyl groups in **6**. Hydrogen atoms bonded to carbon will be included in calculated positions with thermal parameters equal to 1.2 times those of the atoms to which they were bonded. Hydrogen atoms on the water molecules in **3** could not be located. In structures **4**, **7** and **8**, anisotropic thermal parameters for some phenyl rings were constrained to be consistent with ring motion. All structures were corrected for absorption using empirical methods [27]. Difference Fourier maps showed no significant peaks apart from a few close to the heavy atoms. The struc-

tures were then refined on F^2 using SHELX [28]. All calculations were carried out on a Silicon Graphics R4000 Workstation at the University of Reading.

4. Supplementary material

For complexes **1–9**, tables of remaining molecular dimensions not included in this paper, anisotropic and isotropic thermal parameters, and hydrogen coordinates are available. Ordering information is given on any current masthead page. The data have been lodged with the Cambridge Crystallographic Database; CCDC nos. 128908–12916 inclusive.

Acknowledgements

M.M.M. thanks the EPSRC for a studentship. L.A.L. thanks the British Council for providing her with a Research Attachment Award (British Chevening Award) and the University of Malaya for other financial support and leave. U.H. and S.Z. thank the ERASMUS scheme for support. The authors also thank the EPSRC and the University of Reading for funds for the Image Plate System.

References

- [1] J. Lewis, R. Whyman, *J. Chem. Soc.* (1965) 5486.
- [2] M.W. Anker, R. Colton, I.B. Tomkins, *Aust. J. Chem.* 20 (1967) 9.
- [3] J.R. Moss, B.L. Shaw, *J. Chem. Soc. A* (1970) 595.
- [4] B.D. Dombek, R.J. Angelici, *Inorg. Chem.* 15 (1976) 2397.
- [5] S.C. Tripathi, S.C. Srivastava, D.P. Pandey, *Transit. Met. Chem.* 2 (1977) 52.
- [6] P. Umland, H. Vahrenkamp, *Chem. Ber.* 115 (1982) 3555.
- [7] F.A. Cotton, R. Poli, *Inorg. Chem.* 25 (1986) 3703.
- [8] P.K. Baker, S.G. Fraser, *Inorg. Chim. Acta* 116 (1986) L1.
- [9] P.K. Baker, M.A. Beckett, L.M. Severs, *J. Organomet. Chem.* 409 (1991) 213.
- [10] P.K. Baker, D.J.T. Sharp, *J. Coord. Chem.* 16 (1988) 389.
- [11] P.K. Baker, S.G. Fraser, *Inorg. Chim. Acta* 130 (1987) 61.
- [12] P.K. Baker, S.G. Fraser, P. Harding, *Inorg. Chim. Acta* 116 (1986) L5.
- [13] S.C.N. Hsu, W.-Y. Yeh, M.Y. Chaing, *J. Organomet. Chem.* 492 (1995) 121.
- [14] P.K. Baker, S.G. Fraser, M.G.B. Drew, *J. Chem. Soc. Dalton Trans.* (1988) 2729.
- [15] P.K. Baker, E.M. Armstrong, *Polyhedron* 9 (1990) 801.
- [16] P.K. Baker, D.J. Sherlock, *Polyhedron* 13 (1994) 525.
- [17] D. Miguel, J.A. Pérez-Martinez, V. Riera, S. García-Granda, *J. Organomet. Chem.* 455 (1993) 121.
- [18] L. Mihichuk, M. Pizzey, B. Robertson, R. Barton, *Can. J. Chem.* 64 (1986) 991.
- [19] M.G.B. Drew, *Prog. Inorg. Chem.* 23 (1977) 67, and references cited therein.
- [20] M. Melnik, P. Sharrock, *Coord. Chem. Rev.* 65 (1985) 49, and references cited therein.
- [21] P.K. Baker, S.G. Fraser, E.M. Keys, *J. Organomet. Chem.* 309 (1986) 319.
- [22] P.K. Baker, *Adv. Organomet. Chem.* 40 (1996) 45, and references cited therein.
- [23] P.K. Baker, *Chem. Soc. Rev.* 27 (1998) 125, and references cited therein.
- [24] C.A. Tolman, *Chem. Rev.* 77 (1977) 313, and references cited therein.
- [25] W. Kabsch, *J. Appl. Cryst.* 21 (1988) 916.
- [26] G.M. Sheldrick, SHELX86, *Acta Crystallogr. Sect. A* 46 (1990) 467.
- [27] N. Walker, D. Stuart, *Acta Crystallogr. Sect. A* 39 (1983) 158.
- [28] G.M. Sheldrick, SHELXL, 1993, Program for Crystal Structure Refinement, University of Göttingen.